Clinical, laboratory and radiological features predictive of survival in severe COVID-19 in Wuhan, China

Yumei Liu,M.D[1#], Qian Jiang,M.D,Ph.D[2#], Cong Dong,Ph.D[3#], Qin Liu,M.D[4#], Jianjuan Ma,M.D,Ph.D[5#],Xiaoxian Zhang,M.D[2#],Weihua Huang,M.D[3#], Penghui Wu,M.D[3],Changxing Ou,M.D[3], Miaomiao Hu,M.D[1],Jianheng Zhang,M.D[2], Bomeng Zhang, MD[3],Tingting Xia,M.D[4],Lingling Cheng,M.D,Ph.D[2],Xinlu Wang,M.D,Ph.D[4] , Shiyue Li,M.D,Ph.D[2],Qingsi Zeng,M.D,Ph.D[4※],Qingling Zhang,M.D,Ph.D[3※], Kian Fan Chung MD, DSc[6],Haijun Li,M.D[7※], Zhifang Cai,M.D[1※], Jiaxing Xie,M.D,Ph.D[3※]

1 Department of Pulmonary and Critical Care Medicine, Hankou hospital of Wuhan City, Wuhan, China

2 Department of Respiratory Medicine, State Key Laboratory of Respiratory Diseases, National Clinical Research Center for Respiratory Disease, Guangzhou Institute of Respiratory Health, The First Affiliated Hospital of Guangzhou Medical University, Guangzhou, China

3 Department of Allergy and Clinical Immunology, State Key Laboratory of Respiratory Diseases, National Clinical Research Center for Respiratory Disease, Guangzhou Institute of Respiratory Health, The First Affiliated Hospital of Guangzhou Medical University, Guangzhou, China

4 Department of Radiology, The First Affiliated Hospital of Guangzhou Medical University, Guangzhou, China

5 Department of Pediatric Hematology, Affiliated Hospital of Guizhou Medical University, Guizhou,China

6 National Heart & Lung Institute, Imperial College London, London SW3, UK

7 Department of Radiology, Hankou hospital of Wuhan City, Wuhan, China

#The authors contributed equally to this work.

※Correspondence Authors:

1) Jiaxing Xie, M.D,Ph.D

Department of Allergy and Clinical Immunology,

State Key Laboratory of Respiratory Diseases,

National Clinical Research Center for Respiratory Disease,

Guangzhou Institute of Respiratory Health,

The First Affiliated Hospital of Guangzhou Medical University.

Guangzhou, China

Email:jiaxingxie@126.com

2) Zhifang Cai, M.D

Department of Pulmonary and Critical Care Medicine,

Hankou hospital of Wuhan City,

Wuhan, China

Email:caizfang0906@163.com

3) Haijun Li, M.D

Department of Radiology,

Hankou hospital of Wuhan City,

Wuhan, China

Email:lhj03@qq.com

4) Qingling Zhang, M.D,Ph.D

Department of Allergy and Clinical Immunology,

State Key Laboratory of Respiratory Diseases,

National Clinical Research Center for Respiratory Disease,

Guangzhou Institute of Respiratory Health,

The First Affiliated Hospital of Guangzhou Medical University.

Guangzhou, China

Email: qingling@gird.cn

5) Qingsi Zeng, M.D,Ph.D

Department of Radiology,

The First Affiliated Hospital of Guangzhou Medical University,

Guangzhou, China

Email:13660611505@163.com

Abstract

Objectives: We determined the clinical and imaging features of patients with severe COVID-19 that were associated with survival.

Methods: Sixty-seven patients hospitalised with severe laboratory-confirmed COVID-19, were consecutively enrolled. Clinical data, blood measurements and chest computed tomographic (CT) scans were analyzed.

Results: We compared the findings between 39 survivors and 28 non-survivors. At admission, although there were no differences in white blood cell (WBC) and platelet (PLT) counts, there was an increase of WBC, neutrophil, platelet distribution width and mean platelet volume with a marked decrease of lymphocyte, monocyte, eosinophil and PLT in non-survivor group on their last day compared to survivors ($P < 0.05$). Non-survivors had higher ratios of peak creatinine($P<0.05$) and peak lactate dehydrogenase (LDH) ($P<0.05$). Compared to survivors, the incremental rate of total lesion area, ground-glass opacity (GGO) area and consolidation area on CT scans was increased in non-survivors ($P<0.05$).The deceleration rate of total lung volume was greater in non-survivors than survivors($P<0.05$). Using the univariate survival analysis, the following were predictive of non-survival: time from admission to peak of D-dimer (D2D)<16 days , initial pro-BNP>319.0 pg/ml, peak procalcitonin (PCT) ≥0.19 ng/ml, peak creatinine>96.5 μmol/l , median time from admission to peak ALP<18 days, the acceleration rate of total lesional area> -11.5 cm^3/day, incremental rate of GGO area> 2.4 cm^3/day and the acceleration of consolidation area> 2.3 cm^3/day.

Conclusion: Hematological counts, serum analytes and radiological indicators, the latter assessed by artificial intelligence, are robust predictors of survival outcome in COVID-19.

Keywords: COVID-19, CT manifestations, Clinical characteristics, Disease outcome.

Introduction

Since the emergence of SARS-COV-2 in Wuhan, China, in December 2019, this virus has rapidly spread worldwide and has become a global health threat. As of March 30th, 2020, a total of 82,436 confirmed cases had been reported in China, with 3311 deaths. Furthermore, 640,836 confirmed cases, including 30,712 death cases, have been identified in other countries and regions. Due to the lack of medical resources, rapid identification of clinical parameters that are predictive of disease fatality has become critical to reduce death rates. Published studies have indicated that approximately 20% of patients with COVID-19 have been classified as severe or critical. The overall case fatality rate (CFR) has been shown to be 2.3% [1], but this can be as high as 28.2% in severe and critical cases[2]. Previous studies have revealed that older age, being male, comorbidities, a high sequential organ failure assessment (SOFA) score, and increased levels of IL-6, D-dimer, and creatinine are risk factors for COVID-19 mortality [2,3].

Chest computed tomography (CT) plays an essential role in the diagnosis and assessment of the disease severity of COVID-19. According to Chinese management guidelines for COVID-19 (version 7.0)[4], the extent of disease lesions is an indicator of disease severity. Additionally, the presence of ground-glass opacities (GGOs) and consolidation, subpleural lesions, and bilateral lung involvement has also been recognized as classical findings in initial CTs obtained from COVID-19 patients[5-7]. The predominant patterns in the CT images from different time courses in patients with COVID-19 have also been identified[8-10]. However, detailed CT findings of patients with severe or fatal COVID-19 and their associations with clinical features and outcomes have not been extensively reported. Recently, artificial intelligence (AI) has successfully contributed to improving the detection of small pulmonary nodules and other lung diseases[11,12]. Attempts have also been made to differentiate

community acquired pneumonia (CAP) from COVID-19[5,13]. Therefore, AI is becoming a promising technique for characterizing CT images of COVID-19.

The aim of the current study was to evaluate changes associated with chest CT images in patients with severe COVID-19 by using AI and to explore clinical and imaging predictors of disease outcome.

Methods

Ethical approval

This study was performed in accordance with the principles of the Declaration of Helsinki and approved by the ethics committee of the Hankou Hospital in Wuhan City (approval number: hkyy 2020-018). Written informed consent was waived in light of the crisis of the emerging infectious disease.

Clinical data collection

Patients with severe or critical COVID-19 at any time during the disease course were defined as severe. According to the Chinese management guidelines for COVID-19 (version 7.0)[6], severe or critical cases were diagnosed using any one of the following criteria: 1) respiratory rate (RR) ≥ 30 breaths/min; 2) oxygen saturation ≤ 93% at rest; 3) the ratio of arterial partial pressure of oxygen (PaO_2) to the fraction of inspired oxygen (FiO_2) ≤ 300 mmHg (1 mmHg = 0.133 kPa); and 4) the extended size of lesions detected by X-ray and/or CT (≥ 50% in 24–48 hours). Critical status was defined by any one of the following conditions: 1) respiratory failure and a requirement for mechanical ventilation; 2) shock; and 3) concomitant failure of other organs and requirement for intensive care unit (ICU) monitoring and treatment.

All severe COVID-19 adult patients hospitalised between January 26th to February 10th, 2020 in Hankou Hospital of Wuhan City were included . All patients tested positive using reverse-transcriptase polymerase-chain-reaction (RT-PCR) detection of SARS-CoV-2. The demographic and clinical features of each patient, such as age, gender, exposure history, comorbid conditions, symptoms, laboratory results, and diseases outcomes, were collected and analyzed. Patients followed up until March 20th, 2020.

Acquisition and analysis of chest scan images

The frequency of chest CT examinations was determined by the treating physicians. A total of 62 participants had CT exams performed at the time of initial diagnosis, and 50 patients underwent at least one follow-up chest CT. A SIEMENS Definition AS +128 (Siemens Healthineers, Forchheim, Germany) was utilized with 120 kV tube voltage. The slice thickness of images was 1.5 mm in the lung window and 2 mm in the mediastinal window. An artificial intelligence (AI) multi-disciplinary imaging diagnosis platform designed by Yitu Healthcare Company (China) was employed to estimate the extent and morphological features of lesions in patients with severe and fatal COVID-19. First, a deep learning model for AI was developed. The lesion area was then computed and generated by AI **(Figure 1)**. The AI results were then retrospectively reviewed by two experienced radiologists. Lesional volume, distribution pattern, and severity were measured. According to the score of GGO and consolidation lesions that were computed using the weighting function, the degree of involvement was defined as mild, moderate, and severe. Each lobe of the lung was scored using the following formula: 3 × the ratio of consolidation area to the total lobe volume + 2 × the ratio of the GGO area to the total lobe volume. In addition, the entire lung score of each participant was then summed and generated. The acceleration rate of the total lesions, GGO lesions, consolidation lesions, and total lung volume were calculated using the following equation: lesion size of the initial CT – lesion size of the worse CT (if patient had at least three CT examinations) or lesion size of the last CT (if patient only had two CT examinations)/ the duration of selected CT examination.

Statistical analysis

Continuous normally-distributed variables are presented as means ± standard deviations and analyzed using independent t-tests. Continuous non-normally distributed variables were described as medians and interquartile ranges (IQRs) and

assessed using a Mann-Whitney U test. The categorical variables were expressed as frequencies and percentages and evaluated using a Chi-squared test or Fisher's exact test. A univariate survival analysis was used to identify the risk factors for disease mortality. SPSS software version 22.0 (SPSS Inc., Chicago, IL, USA) was used for the statistical analysis. A two-sided P value less than 0.05 was considered to be significant.

Results

Clinical characteristics of survivors and non-survivors

Sixty-seven patients with COVID-19, including 39 survivors and 28 non-survivors, hospitalized at Hankou hospital of Wuhan City were included, with a mortality rate of 41.8% (28/67) **(Table 1)**. There was no gender bias or age differences between survivors and non-survivors. 45 out of the 67 patients (67.1%) had a comorbid condition, with hypertension (38.8%) being the most common, followed by diabetes (23.9%), cardiovascular diseases (19.4%), cerebrovascular diseases (4.5%), and cancer (4.5%). The proportion of patients with at least one comorbidity was higher in the non-survivor group (78.6% vs. 60.0%), but there was no statistically difference ($P = 0.295$). The most frequent symptoms of COVID-19 were fever (92.5%), cough (85.1%), breathlessness (80.6%), sputum (61.2%), fatigue (47.8%), and diarrhea (10.4%) with the incidence of hypoxemia being high in both non-survivors (100%) and survivors (92.3%).

At the time of admission, white blood cell (WBC), neutrophil (NEU), lymphocyte (LYM), eosinophil (EOS), monocyte (MON), and platelet (PLT) counts, platelet distribution width (PDW) and mean platelet volume (MPV) were not significantly different between survivors and non-survivors. However, compared to the survivor group, there were higher WBC, NEU, PDW and MPV and a marked decrease of LYM, MON, EOS and PLT in the non-survivor group at the time of end hospitalization ($P < 0.05$) **(Figure 2)**. In addition, the proportion of LYM in non-survivor group [Median(IQR):4.2%(3.4%-6.62%)] was lower than that in survivor group

[Median(IQR):9.9%(4.9%-19.3%)] during the middle of hospitalization ($P < 0.05$) **(Figure 2)**. Non-survivors presented with higher levels of NEU to LYM ratio (NLR), PLT to LYM ratio (PLR) and MPV to PLT ratio (MPR) ($P < 0.05$) **(Supplementary Figure 1)**.The laboratory findings of the subjects are presented in **Table 2**. The peak levels of creatinine and lactate dehydrogenase (LDH) measured after admission were markedly higher in the non-survivor group ($P < 0.05$), indicating the involvement of multiple organs. Although no significant difference in D-dimer was found between the two groups, time from admission to the peak of D-dimer was significantly shorter in non-survivors ($P < 0.05$). Increasing trends in pro B-type natriuretic peptide (BNP), procalcitonin (PCT), alanine aminotransferase (ALT), aspartate aminotransferase (AST), total bilirubin (TB), direct bilirubin (DBIL), and C-reactive protein (CRP) were also observed in non-survivors compared with that in survivors.

Corticosteroid treatment was utilized in 94.8% (37/39) of survivors and 89.3% (25/28) of non-survivors in this study. The timing, total dosage, and duration of steroid treatment did not differ between the two groups **(Table 3)**. A total of 27 of 38 survivors and 16 of 25 non-survivors in this study received oseltamivir treatment. Additionally, oseltamivir and biphasic positive airway pressure (BiPAP) were frequently-used therapeutic options for severe COVID-19 patients. Compared with survivors, more non-survivors underwent non-invasive ventilation ($P < 0.05$), suggesting respiratory failure was more common in non-survivors **(Table 3)**.

Findings of the chest CT scan

The progression of lesional areas, including total lesional area, GGO lesional area, and consolidation lesional area, are shown in **Figure 3A–F.** A majority of the non-survivor group underwent only one CT examination during the course of the disease. The maximal lesional area of the chest CT in the survivor group was distributed over 8–14 days (time from initial symptoms to the CT examination). As the disease progressed, the lesional areas in most of the survivors did not present a gradually decreasing tendency, with the exception of the consolidation lesion area,

which showed a dramatic decrease during the course of the disease. However, there was no obvious increasing tendency in the lesional area in the non-survivor group.

To study the chest CT in patients with severe COVID-19, the CT scans were grouped according to a timeline after the occurrence of initial symptoms defined as: stage 1 (1–7 days after symptom onset), stage 2 (8–14 days after symptom onset), and stage 3 (15–21 days after symptom onset). As shown in **Table 4**, the severity of the lesions in the chest CT progressed stage by stage (from 50% in stage 1 to 95% in stage 3). GGOs and consolidation were the most common CT findings in non-surviving COVID-19 patients. More than 60% of the patients with fatal COVID-19 displayed GGO involvement in five lobes, and 20% showed consolidation in at least two lobes **(Table 4)**.

Although no significant difference was found in the total lesional area and the GGO lesional areas between the two groups, the increasing trend during these stages was more obvious in non-survivors [from (700.7 ± 739.0) cm^3 and (585.1 ± 650.6) cm^3 at stage 1 to (1494.9 ± 1028.8) cm^3 and (1275.2 ± 943.4) cm^3 at stage 3 than that in survivors [from (718.5 ± 526.4) cm^3 and (566.4 ± 409.9) cm^3 at stage 1 to (1228.7 ± 673.2) cm^3 and (937.8 ± 593.6) cm^3 at stage 3] **(Figure 4A-B)**. Interestingly, the falling trend of the consolidation lesions was more pronounced in the survivor group in comparison with the non-survivor group **(Figure 4C)**. At stage 1, the consolidation lesion area in the non-survivors was significantly lower than that in the survivors **(Figure 4C)** ($P < 0.05$). The total CT scores did not differ between the two groups during the course of the disease **(Figure 4D)**.

CT images of a non-survivor and a survivor are presented in **Figure 5A–H**. The acceleration rates of the total lesion area, GGO area, consolidation area, and total lung volume were also computed during the course of the disease **(Figure 6A–D)**. Compared with the survivors, the acceleration rates of the total lesion area, GGO area, and consolidation area were significantly elevated in the non-survivors ($P < 0.05$). Moreover, the deceleration of the total lung volume in the non-survivor group (-109.6 ± 86.3) cm^3/day was more obvious than that in the survivor group (-12.4 ± 65.4)

cm^3/day ($P < 0.05$). An increase in the lesional area and a decrease in the total lung volume were implicated during the process of COVID-19. There was a significant positive correlation between the acceleration of consolidated area and acceleration of GGO area, and inverse correlation between the deceleration of total lung volume and acceleration of GGO area, and between the deceleration of total lung volume and acceleration of consolidation area (**Figure 7**).

Factors predictive of poor prognosis

To identify predictors of disease outcomes, univariate survival analysis was performed. The following parameters were associated with an increased risk of disease fatality. The median time from admission to the peak of D-dimer < 16 days ($P < 0.05$), an initial pro-BNP>319.0pg/ml ($P < 0.05$), a peak PCT≥0.19 ng/ml ($P < 0.05$), a peak creatinine > 96.5 μmol/l ($P < 0.05$), the median time from admission to the peak of ALP < 18 days ($P < 0.05$), the median time from admission to the peak of ALT < 17 days ($P < 0.05$), an elevated acceleration of the total lesion area > -11.5 cm^3/day ($P < 0.05$), an elevated acceleration of the GGO area > 2.4 cm^3/day ($P < 0.05$), and an increase in the speed of the consolidation area > 2.3 cm^3/day ($P < 0.05$) **(Figure 8 A–F and Figure 9 A–C)**.

Discussion

At present, supportive care remains the primary treatment option for patients with severe or fatal COVID-19 because there are no specific anti-viral therapies for COVID-19. Early detection and supportive treatment of patients who are likely to have fatal outcomes are important and likely to reduce the mortality rate. The clinical course and features of patients with COVID-19 have been discussed [1,14-17]. However, the imaging and clinical characteristics of subjects with severe and fatal COVID-19 and their impacts on disease outcomes have not been well reported, particular in the use of artificial intelligence to evaluate the lung lesional distribution in these patients.

In our study, the clinical course of non-survivors was confirmed to be markedly shorter than that of survivors (10.5 days vs. 34.0 days), indicating the possibility of a rapid deterioration in lung involvement. A quick and effective treatment strategy is needed for patients with severe and fatal COVID-19. The baseline characteristics of blood cell counts in participants were consistent in the current study, indicating homogeneity of the patients studied. Consistent with previous findings[18-21], in which the increase of WBC, NEU, Neutrophil/Lymphocyte Ratio (NLR) and Platelet /Lymphocyte Ratio (PLR) and the decrease of LYM have been reported to be associated with disease severity of SARS and COVID-19, a decrease in LYM and PLT and an increase in NEU, NLR and PLR was more obvious in non-survivors, suggesting a dysregulation of the immune system. Platelet distribution width (PDW) and mean platelet volume (MPV) have been shown to be independent risks factors for venous thromboembolic disease (VTE) [22], bacteremia[23] and influenza A infection[24]. However, their implication in COVID-19 has not been reported. In this study, the PDW and MPV were much higher in the non-survivors than that in survivors at the time of end hospitalization, suggesting that these may contribute to the lethal outcome. Pathological findings of extrapulmonary organ damage in the late stage of COVID-19, including cardiac injury, acute kidney injury, acute liver injury, and an impaired coagulation system, have been reported [25,26]. Similar to previous studies[27,28], the involvement of cardiac (with high levels of LDH), kidney (increase of creatinine), liver (upregulation of TB, DBIL, ALT, AST, and ALP), the coagulation system (rise of FIB and D2D), and the immune system (imbalance in LYM and NEU) was observed in patients with severe and fatal COVID-19. The use of a comprehensive multi-organ monitoring plan in these COVID-19 patients is crucial.

AI was employed for the first time in this study to evaluate the features of CT imaging in patients with severe COVID-19. According to the time-line of the lesional area measured by AI, patients with severe COVID-19 were assigned to three groups. The acceleration rate in the total lesions, GGO lesions, and consolidation lesions was lower in the non-survivors than that in the survivors. However, inconsistent with

previous findings[8], an obvious and marked dynamic change in the CT score was not found during the recovery of COVID-19. There are several reasons for this. First, the scoring system used was different between these studies. Second, the CT images included in the current study were not paired and often only one CT was performed. Third, the majority of non-survivors had only one CT examination.

GGO was the primary morphologic lesion in this study, followed by consolidation. Diffuse alveolar damage corresponds to the occurrence of GGO in viral pneumonia[29,30]. The proportion of severe and fatal COVID-19 patients with GGO involvement in the five lobes was fairly high in this study, which can also underlie the increased incidence of hypoxemia in these COVID-19 patients. Although the typical dynamic changes in the GGO lesion area were absent in non-survivors, an obvious increased speed of the GGO lesional area in these patients was found. In addition, patients with the increased acceleration in the GGO area of more than 2.4 cm^3/day had a worse clinical outcome.

Consolidation are not only found in CT images of various viral pneumonias, but they have also been confirmed as a marker of bacterial-superimposed infection in viral and fungal pneumonia[29,31]. More than 30% of fatal H1N1 patients had bacterial-superimposed infections during the evolution of H1N1[32]. It was discovered in this study that the consolidation lesion area in non-survivors was significantly lower than that in survivors at stage 1. During the evolution of COVID-19, the acceleration rate of consolidation lesions was remarkably increased in non-survivors compared with that in survivors. The consolidation area also decreased stage by stage in the survivors. Additionally, the PCT level was also up-regulated in non-survivors, indicating that bacterial-superimposed infection may contribute to a worse clinical outcome. Using a univariate survival analysis, the increased speed of the total lesion area and consolidation area were identified as initial strong indicators of clinical outcome.

There are limitations in this study. The sample size was small. The examination of the chest CT scans were not paired between the survivors and the non-survivors. The

AI technique we used was still being improved to work as a discriminator between the morphology of lesions. The multivariable logistic regression analysis was incomplete due to the small sample size, rendered even smaller by a lot of patients who did not have a second CT scan and by missing data. A larger sample size study should be studied to confirm the results of this study.

In conclusion, hematological indicators including lymphocyte, lymphocyte percentage, and neutrophil to lymphocyte ratio, the median time from admission to the peak of D2D and BNP, PCT, and creatinine and the rapid appearance of total lesion area, GGO area, and consolidation area are robust predictors of disease outcomes in COVID-19. These findings will help to further improve the management of COVID-19 patients.

Acknowledgments

We acknowledge the dedication of all healthcare workers involved in the diagnosis and treatment of COVID-19 patients in Hankou Hospital, Wuhan City. We deeply thank Dr. Ying Huang for the preparation of this manuscript.

This work was supported in part by the grants from the Natural Science Foundation of Guangdong Province (Grant No.2019A1515010622, 2017A030310267), the Foundation for High-Level University Construction of the Guangzhou Medical University (Professor Kian Fan Chung project, Grant No.B195002010041), and the Precision Medicine Research of the National Key Research and Development Plan of China (Grant No. 2016YFC0905800).

Declaration of interest

The authors have declared no conflicts of interest and are responsible for the content of this manuscript.

Reference:

1. [The epidemiological characteristics of an outbreak of 2019 novel coronavirus diseases (COVID-19) in China]. *Zhonghua Liu Xing Bing Xue Za Zhi.* 2020;41(2):145-151
2. Zhou F, Yu T, Du R, Fan G, Liu Y, Liu Z, Xiang J, Wang Y, Song B, Gu X, Guan L, Wei Y, Li H, Wu X, Xu J, Tu S, Zhang Y, Chen H, Cao B. Clinical course and risk factors for mortality of adult inpatients with COVID-19 in Wuhan, China: a retrospective cohort study. *Lancet.* 2020;395(10229):1054-1062
3. Caramelo F, Ferreira N, Oliveiros B. Estimation of risk factors for COVID-19 mortality - preliminary results. *medRxiv.* 2020:2020.2002.2024.20027268
4. National Health Commission of the People's Republic of China.Chinese management guideline for COVID-19 (version 7.0). *Clinical Education of General Practice.*18(2):100-105
5. Ai T, Yang Z, Hou H, Zhan C, Chen C, Lv W, Tao Q, Sun Z, Xia L. Correlation of Chest CT and RT-PCR Testing in Coronavirus Disease 2019 (COVID-19) in China: A Report of 1014 Cases. *Radiology.* 2020:200642
6. Xiong Y, Sun D, Liu Y, Fan Y, Zhao L, Li X, Zhu W. Clinical and High-Resolution CT Features of the COVID-19 Infection: Comparison of the Initial and Follow-up Changes. *Invest Radiol.* 2020
7. Xu X, Yu C, Qu J, Zhang L, Jiang S, Huang D, Chen B, Zhang Z, Guan W, Ling Z, Jiang R, Hu T, Ding Y, Lin L, Gan Q, Luo L, Tang X, Liu J. Imaging and clinical features of patients with 2019 novel coronavirus SARS-CoV-2. *Eur J Nucl Med Mol Imaging.* 2020;47(5):1275-1280
8. Pan F, Ye T, Sun P, Gui S, Liang B, Li L, Zheng D, Wang J, Hesketh RL, Yang L, Zheng C. Time Course of Lung Changes On Chest CT During Recovery From 2019 Novel Coronavirus (COVID-19) Pneumonia. *Radiology.* 2020:200370
9. Bernheim A, Mei X, Huang M, Yang Y, Fayad ZA, Zhang N, Diao K, Lin B, Zhu X, Li K, Li S, Shan H, Jacobi A, Chung M. Chest CT Findings in Coronavirus Disease-19 (COVID-19): Relationship to Duration of Infection. *Radiology.* 2020:200463
10. Shi H, Han X, Jiang N, Cao Y, Alwalid O, Gu J, Fan Y, Zheng C. Radiological findings from 81 patients with COVID-19 pneumonia in Wuhan, China: a descriptive study. *Lancet Infect Dis.* 2020;20(4):425-434
11. Li X, Guo F, Zhou Z, Zhang F, Wang Q, Peng Z, Su D, Fan Y, Wang Y. [Performance of Deep-learning-based Artificial Intelligence on Detection of Pulmonary Nodules in Chest CT]. *Zhongguo Fei Ai Za Zhi.* 2019;22(6):336-340
12. Fischer AM, Varga-Szemes A, van Assen M, Griffith LP, Sahbaee P, Sperl JI, Nance JW, Schoepf UJ. Comparison of Artificial Intelligence-Based Fully Automatic Chest CT Emphysema Quantification to Pulmonary Function Testing. *AJR Am J Roentgenol.* 2020:1-7
13. Li L, Qin L, Xu Z, Yin Y, Wang X, Kong B, Bai J, Lu Y, Fang Z, Song Q, Cao K, Liu D, Wang G, Xu Q, Fang X, Zhang S, Xia J, Xia J. Artificial Intelligence Distinguishes COVID-19 from Community Acquired Pneumonia on Chest CT. *Radiology.* 2020:200905
14. Guan WJ, Ni ZY, Hu Y, Liang WH, Ou CQ, He JX, Liu L, Shan H, Lei CL, Hui DSC, Du B, Li LJ, Zeng G, Yuen KY, Chen RC, Tang CL, Wang T, Chen PY, Xiang J, Li SY, Wang JL, Liang ZJ, Peng YX, Wei L, Liu Y, Hu YH, Peng P, Wang JM, Liu JY, Chen Z, Li G,

Zheng ZJ, Qiu SQ, Luo J, Ye CJ, Zhu SY, Zhong NS. Clinical Characteristics of Coronavirus Disease 2019 in China. *N Engl J Med.* 2020

15. Wu J, Liu J, Zhao X, Liu C, Wang W, Wang D, Xu W, Zhang C, Yu J, Jiang B, Cao H, Li L. Clinical Characteristics of Imported Cases of COVID-19 in Jiangsu Province: A Multicenter Descriptive Study. *Clin Infect Dis.* 2020
16. Yang W, Cao Q, Qin L, Wang X, Cheng Z, Pan A, Dai J, Sun Q, Zhao F, Qu J, Yan F. Clinical characteristics and imaging manifestations of the 2019 novel coronavirus disease (COVID-19):A multi-center study in Wenzhou city, Zhejiang, China. *J Infect.* 2020;80(4):388-393
17. Zhang JJ, Dong X, Cao YY, Yuan YD, Yang YB, Yan YQ, Akdis CA, Gao YD. Clinical characteristics of 140 patients infected with SARS-CoV-2 in Wuhan, China. *Allergy.* 2020
18. Qin C, Zhou L, Hu Z, Zhang S, Yang S, Tao Y, Xie C, Ma K, Shang K, Wang W, Tian DS. Dysregulation of immune response in patients with COVID-19 in Wuhan, China. *Clin Infect Dis.* 2020
19. Wang D, Hu B, Hu C, Zhu F, Liu X, Zhang J, Wang B, Xiang H, Cheng Z, Xiong Y, Zhao Y, Li Y, Wang X, Peng Z. Clinical Characteristics of 138 Hospitalized Patients With 2019 Novel Coronavirus-Infected Pneumonia in Wuhan, China. *Jama.* 2020
20. Fan BE, Chong VCL, Chan SSW, Lim GH, Lim KGE, Tan GB, Mucheli SS, Kuperan P, Ong KH. Hematologic parameters in patients with COVID-19 infection. *Am J Hematol.* 2020
21. Deng Y, Liu W, Liu K, Fang YY, Shang J, Zhou L, Wang K, Leng F, Wei S, Chen L, Liu HG. Clinical characteristics of fatal and recovered cases of coronavirus disease 2019 (COVID-19) in Wuhan, China: a retrospective study. *Chin Med J (Engl).* 2020
22. Diaz JM, Boietti BR, Vazquez FJ, Waisman GD, Giunta DH, Rojas LP, Peuchot V, Posadas-Martinez ML. Mean platelet volume as a prognostic factor for venous thromboembolic disease. *Rev Med Chil.* 2019;147(2):145-152
23. Djordjevic D, Rondovic G, Surbatovic M, Stanojevic I, Udovicic I, Andjelic T, Zeba S, Milosavljevic S, Stankovic N, Abazovic D, Jevdjic J, Vojvodic D. Neutrophil-to-Lymphocyte Ratio, Monocyte-to-Lymphocyte Ratio, Platelet-to-Lymphocyte Ratio, and Mean Platelet Volume-to-Platelet Count Ratio as Biomarkers in Critically Ill and Injured Patients: Which Ratio to Choose to Predict Outcome and Nature of Bacteremia? *Mediators Inflamm.* 2018;2018:3758068
24. Fei Y, Zhang H, Zhang C. The application of lymphocyte*platelet and mean platelet volume/platelet ratio in influenza A infection in children. *J Clin Lab Anal.* 2019;33(9):e22995
25. Xu Z, Shi L, Wang Y, Zhang J, Huang L, Zhang C, Liu S, Zhao P, Liu H, Zhu L, Tai Y, Bai C, Gao T, Song J, Xia P, Dong J, Zhao J, Wang FS. Pathological findings of COVID-19 associated with acute respiratory distress syndrome. *Lancet Respir Med.* 2020;8(4):420-422
26. Liu J, Zheng X, Tong Q, Li W, Wang B, Sutter K, Trilling M, Lu M, Dittmer U, Yang D. Overlapping and discrete aspects of the pathology and pathogenesis of the emerging human pathogenic coronaviruses SARS-CoV, MERS-CoV, and 2019-nCoV. *J Med Virol.* 2020;92(5):491-494
27. Clinical characteristics of 113 deceased patients with coronavirus disease 2019:

retrospective study. *Bmj*. 2020;368:m1295

28. Zhang G, Zhang J, Wang B, Zhu X, Wang Q, Qiu S. Analysis of clinical characteristics and laboratory findings of 95 cases of 2019 novel coronavirus pneumonia in Wuhan, China: a retrospective analysis. *Respir Res.* 2020;21(1):74
29. Koo HJ, Lim S, Choe J, Choi SH, Sung H, Do KH. Radiographic and CT Features of Viral Pneumonia. *Radiographics.* 2018;38(3):719-739
30. Chong S, Kim TS, Cho EY. Herpes simplex virus pneumonia: high-resolution CT findings. *Br J Radiol.* 2010;83(991):585-589
31. Chen W, Xiong X, Xie B, Ou Y, Hou W, Du M, Chen Y, Chen K, Li J, Pei L, Fu G, Liu D, Huang Y. Pulmonary invasive fungal disease and bacterial pneumonia: a comparative study with high-resolution CT. *Am J Transl Res.* 2019;11(7):4542-4551
32. Wright PF, Kirkland KB, Modlin JF. When to consider the use of antibiotics in the treatment of 2009 H1N1 influenza-associated pneumonia. *N Engl J Med.* 2009;361(24):e112

Abbreviation list

COVID-19	Corona Virus Disease-19
2019-nCoV	2019 novel coronavirus
NEU	Neutrophil
LYM	lymphocyte
NLR	the ratio of NEU to lymphocyte
TB	total bilirubin
pro-BNP	B-type natriuretic peptide
LDH	lactate dehydrogenase
D2D	D-dimer
GGO	ground-glass opacities
PCT	procalcitonin
ALP	alkaline phosphatase
CFR	case fatality rate
SOFA	sequential organ failure assessment
CT	computed tomography
AI	artificial intelligence
CAP	acquired pneumonia
RR	respiratory rate
PaO2	arterial partial pressure of oxygen
ICU	intensive care unit
RT-PCR	reverse-transcriptase polymerase-chain-reaction
IQR	interquartile range
ALT	alanine aminotransferase
AST	aspartate aminotransferase
DBIL	direct bilirubin
CRP	C-reactive protein
BiPAP	biphasic positive airway pressure
WBC	white blood cell
PLT	platelet
PDW	platelet distribution width
MPV	mean platelet volume
RDW-SD	red blood cell distribution width-standard deviation
RDW-CV	red blood cell distribution width-coefficient of variation

Figure legends:

Figure 1. **Artificial Intelligence operation in one Computed Tomogram (CT) of the lungs**. A) Density analysis of both lungs on CT; B) Cross-sectional CT image C) List of lesions in each lobe D) Overall results of ground glass opacity (GGO), consolidation and total (lesion) areas; E) A heat map of the lesions: for the inflammatory annotation of the image, mixed density lesions were distinguished according to the depth of the color. Lesions with a CT value less than -500 HU are indicated as light blue, between -500 HU and -250 HU (dark blue) and above -250 HU (deep red); and F) Inflammatory density analysis was employed to evaluate the CT value of the affected tissue, presented as a histogram.

Figure 2. Hematological changes of survivors and non-survivors at the end-hospitalization point including A) lymphocyte counts, B) lymphocyte percentage, C) eosinophil counts, D) eosinophil percentage, F) monocyte percentage, G) platelet counts, H) red blood cell distribution width-standard deviation (RDW-SD), I) red blood cell distribution width-coefficient of variation (RDW-CV) J) white blood cell counts, K) neutrophil counts, H) neutrophil percentage, M) platelet distribution width (PDW), N) mean platelet volume (MPV) measured at time of admission (TA), at mid-hospitalization (TMH) and at end-hospitalization (THE). Data shown for all those who had measurements at the 3 time-points. Statistical significance by Kruskal-Wallis test: # $P < 0.05$, ## $P < 0.01$, ### $P < 0.001$ represented TMH and THE compared with TA; † $P < 0.05$, ‡ $P < 0.01$, § $P < 0.001$ represented THE compared with TA. * $P < 0.05$, ** $P < 0.01$, ***$P < 0.001$ for comparison at the same point.

Figure 3. **Time course of lesional areas on chest CT from symptom onset to CT examination.** (A & B) Changes in total lesional area; (C& D) Changes in the GGO area ; (D & E) The alterations in the consolidation area in survivors and non-survivors, respectively. The lesional areas (cm^3) are expressed as $\log_{10}$.

Figure 4. Lesional areas and total lung volume of the CT imaging in three stages. A)

Changes in total lesional area; B) Aalternations in the GGO lesional area; C) Variations in the consolidation area; D) total CT score. Individual data points with mean ± standard deviation. * $p<0.05$.

Figure 5. Chest CT images in a survivor and a non-survivor. A 58-year-old male patient in the survivor group: Panels A and B at 4 days after symptom onset showing solid shadowing and ground glass opacity (GGO) present in the right and left upper lobes; Panels C and D, 16 days after symptom onset, showing an obvious increase in multiple lesions, especially GGO lesions distributed in both lungs. A 68-year-old female patient who was a non-survivor : Panels E and F, 4 days after symptom onset, with solid shadow and GGO in both lower lobes; Panels G and H, 16 days after symptom onset, with an evident increase in the multiple lesions, especially GGOs, distributed in the both lungs.

Figure 6. The speed of the progression of A) the total lesion areas; B) GGO area; C) consolidation area; D) total lung volume between the survivors and non-survivors. Data presented as individual points with mean ± standard deviation; * $p< 0.05$.

Figure 7. Correlation between the acceleration of consolidated area and acceleration of GGO area (A), the deceleration of total lung volume and acceleration of GGO area (B), and the deceleration of total lung volume and acceleration of consolidation area (C).

Figure 8. Survival curves associated with different serum measurements. A) Initial pro-BNP; B) peak ALP; C) peak creatinine; D) the median time from admission to the peak of D-dimer; E) peak PCT; F) the median time from admission to the peak of ALT.

Figure 9. Survival curves associated with chest CT scan features. A) the

acceleration of total lesion area; B) the acceleration of the GGO area; and C) the acceleration of the consolidation area.

A

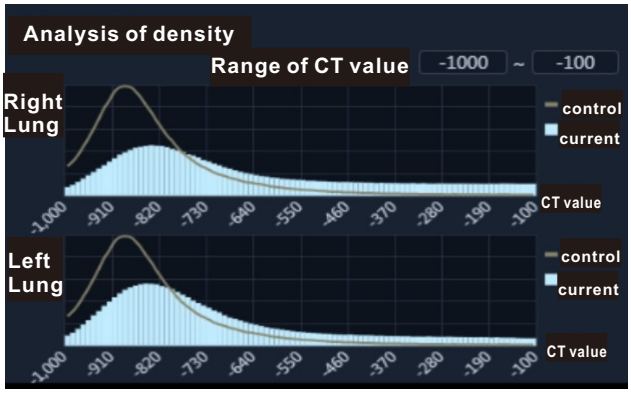

B

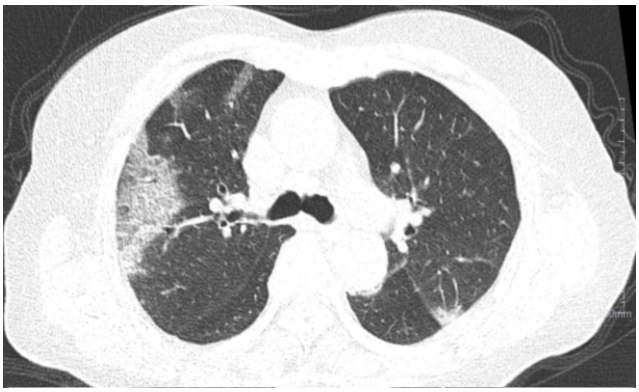

C

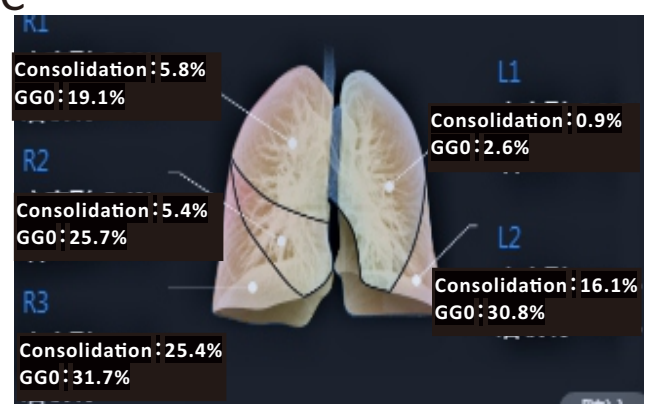

D

	Bilateral (%)	Right (%)	Left (%)	Bilateral (cm^3)	Right (cm^3)	Left (cm^3)
Lesion	31.13	39.28	21.34	852.37	586.77	265.59
GGO	20.42	25.61	14.2	559.26	382.53	176.73
Consolidation	10.7	13.67	7.14	293.1	204.24	88.86
Total	-	-	-	2738.28	1493.67	1244.6

E

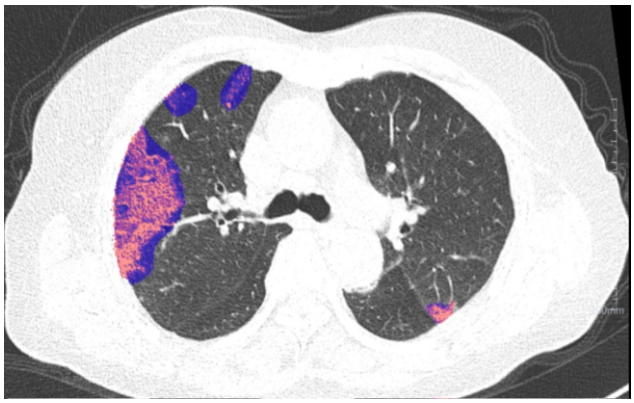

F

Figure 1

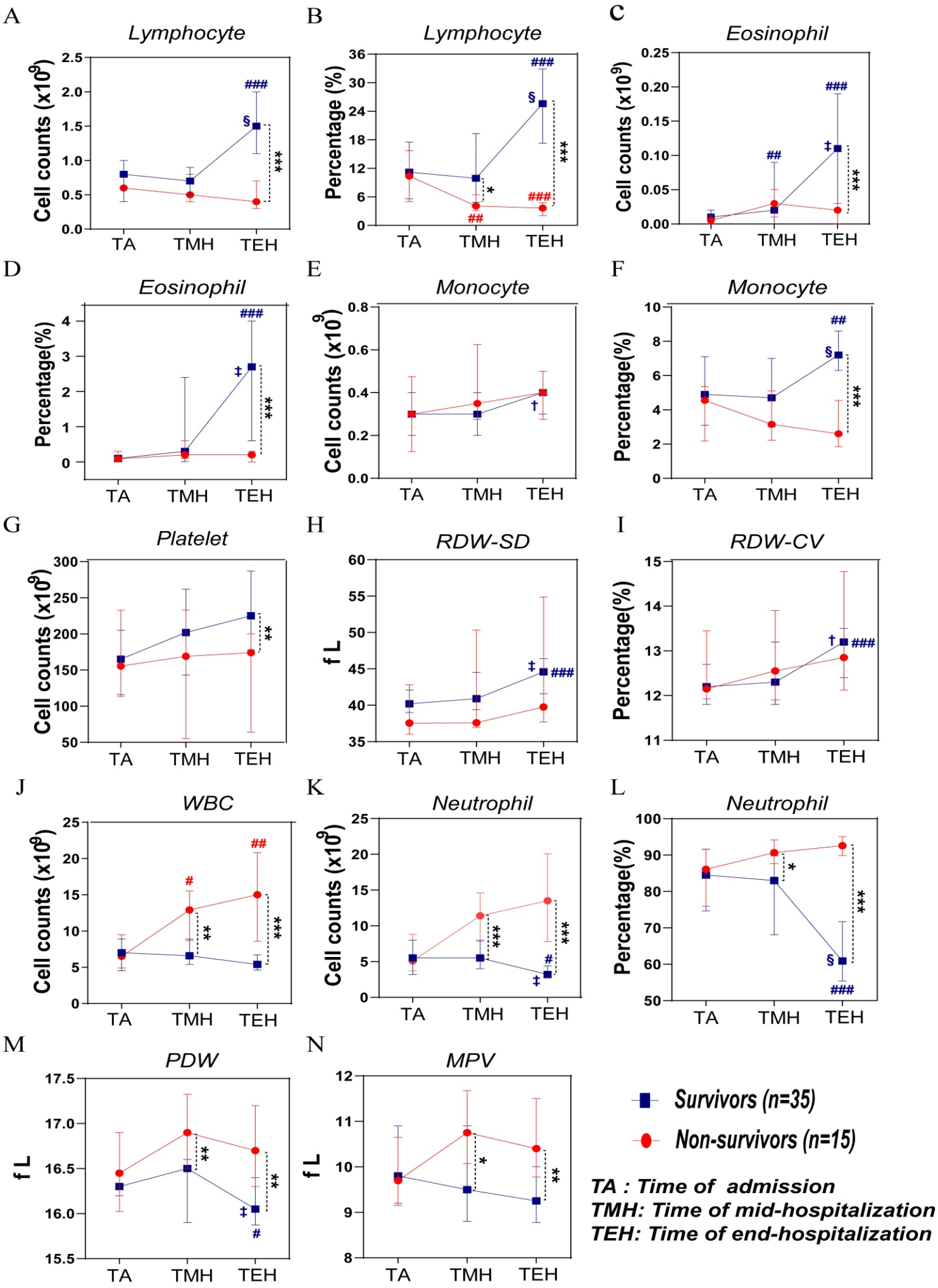
Hematological characteristics of survivors and non-survivors
A
Lymphocyte
Cell counts (x10^9)
B
Lymphocyte
Percentage (%)
C
Eosinophil
Cell counts (x10^9)
D
Eosinophil
Percentage(%)
E
Monocyte
Cell counts (x10^9)
F
Monocyte
Percentage(%)
G
Platelet
Cell counts (x10^9)
H
RDW-SD
f L
I
RDW-CV
Percentage(%)
J
WBC
Cell counts (x10^9)
K
Neutrophil
Cell counts (x10^9)
L
Neutrophil
Percentage(%)
M
PDW
f L
N
MPV
f L
TA
TMH
TEH
Survivors (n=35)
Non-survivors (n=15)
TA : Time of admission
TMH: Time of mid-hospitalization
TEH: Time of end-hospitalization

Figure 2

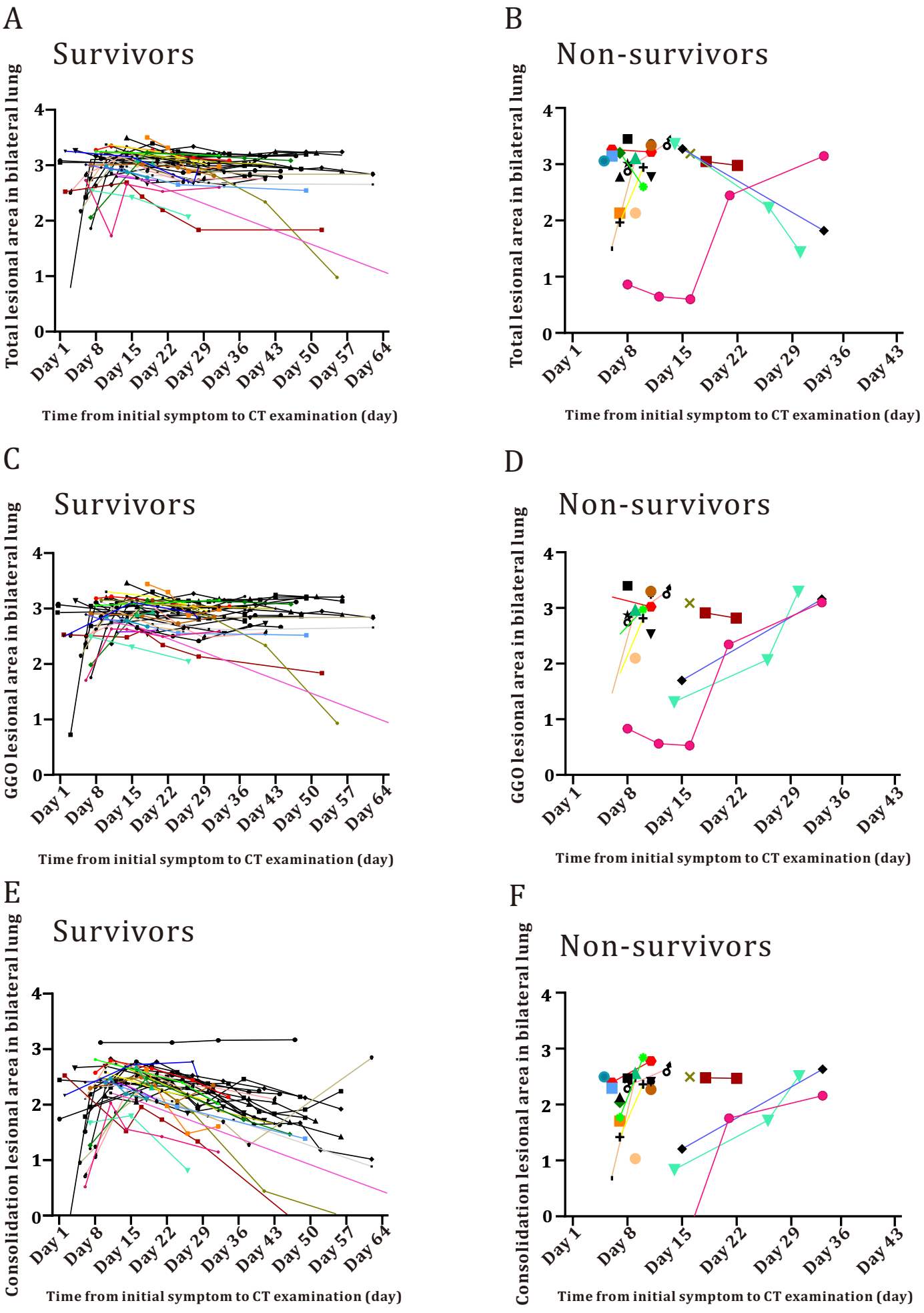
A
Survivors
Total lesional area in bilateral lung
Time from initial symptom to CT examination (day)
B
Non-survivors
Total lesional area in bilateral lung
Time from initial symptom to CT examination (day)
C
Survivors
GGO lesional area in bilateral lung
Time from initial symptom to CT examination (day)
D
Non-survivors
GGO lesional area in bilateral lung
Time from initial symptom to CT examination (day)
E
Survivors
Consolidation lesional area in bilateral lung
Time from initial symptom to CT examination (day)
F
Non-survivors
Consolidation lesional area in bilateral lung
Time from initial symptom to CT examination (day)
0
1
2
3
4
Day 1
Day 8
Day 15
Day 22
Day 29
Day 36
Day 43
Day 50
Day 57
Day 64

Figure 3

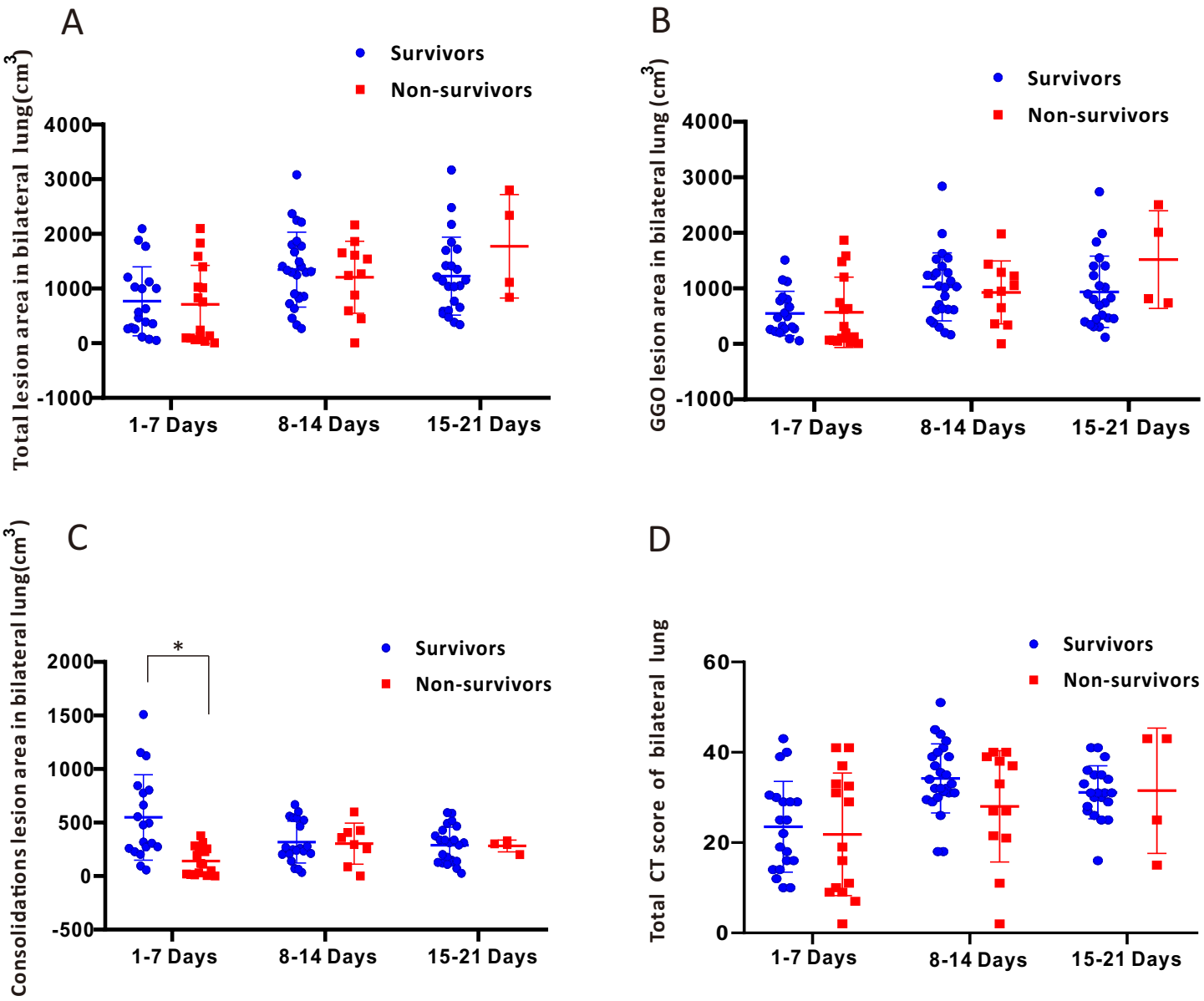
A
Survivors
Non-survivors
Total lesion area in bilateral lung(cm3)
4000
3000
2000
1000
0
-1000
1-7 Days
8-14 Days
15-21 Days
B
Survivors
Non-survivors
GGO lesion area in bilateral lung (cm3)
4000
3000
2000
1000
0
-1000
1-7 Days
8-14 Days
15-21 Days
C
*
Survivors
Non-survivors
Consolidations lesion area in bilateral lung(cm3)
2000
1500
1000
500
0
-500
1-7 Days
8-14 Days
15-21 Days
D
Survivors
Non-survivors
Total CT score of bilateral lung
60
40
20
0
1-7 Days
8-14 Days
15-21 Days

Figure 4

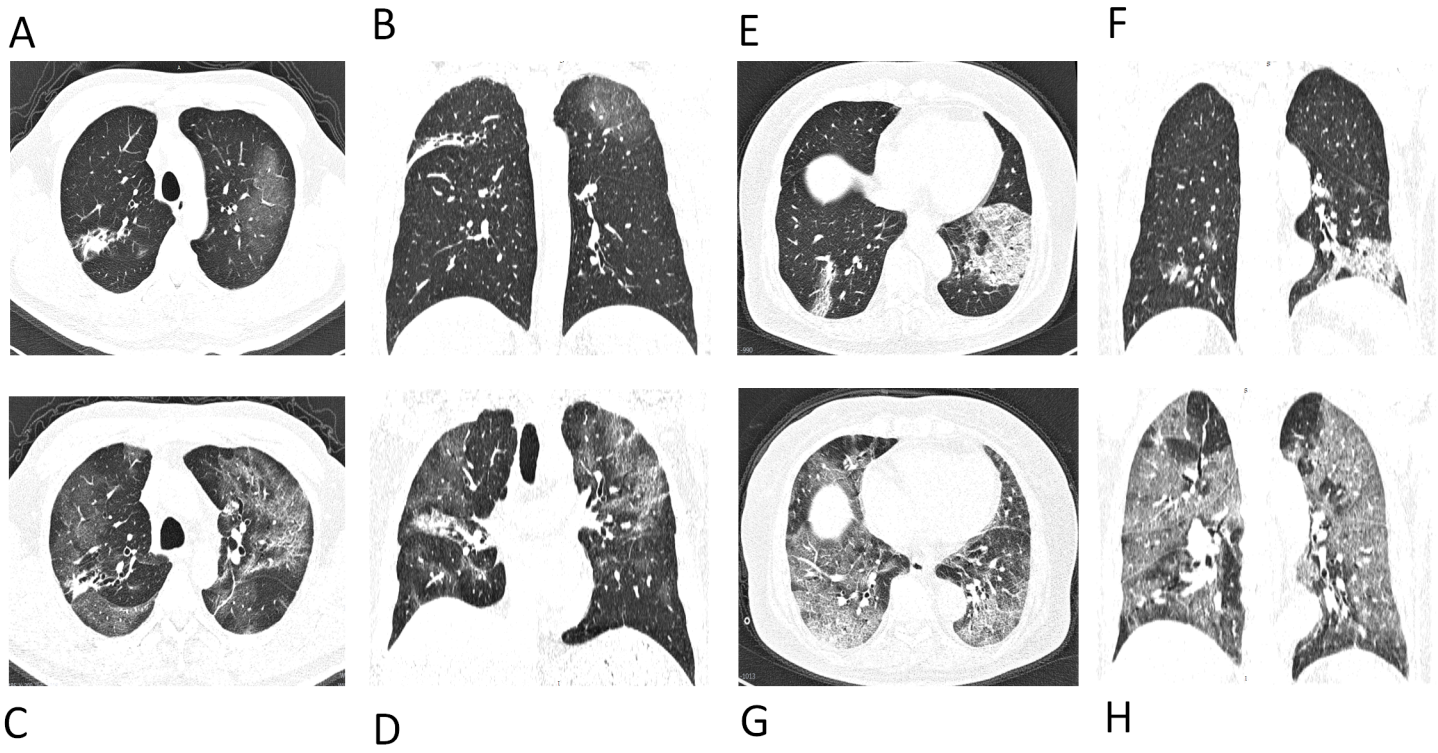

Figure 5

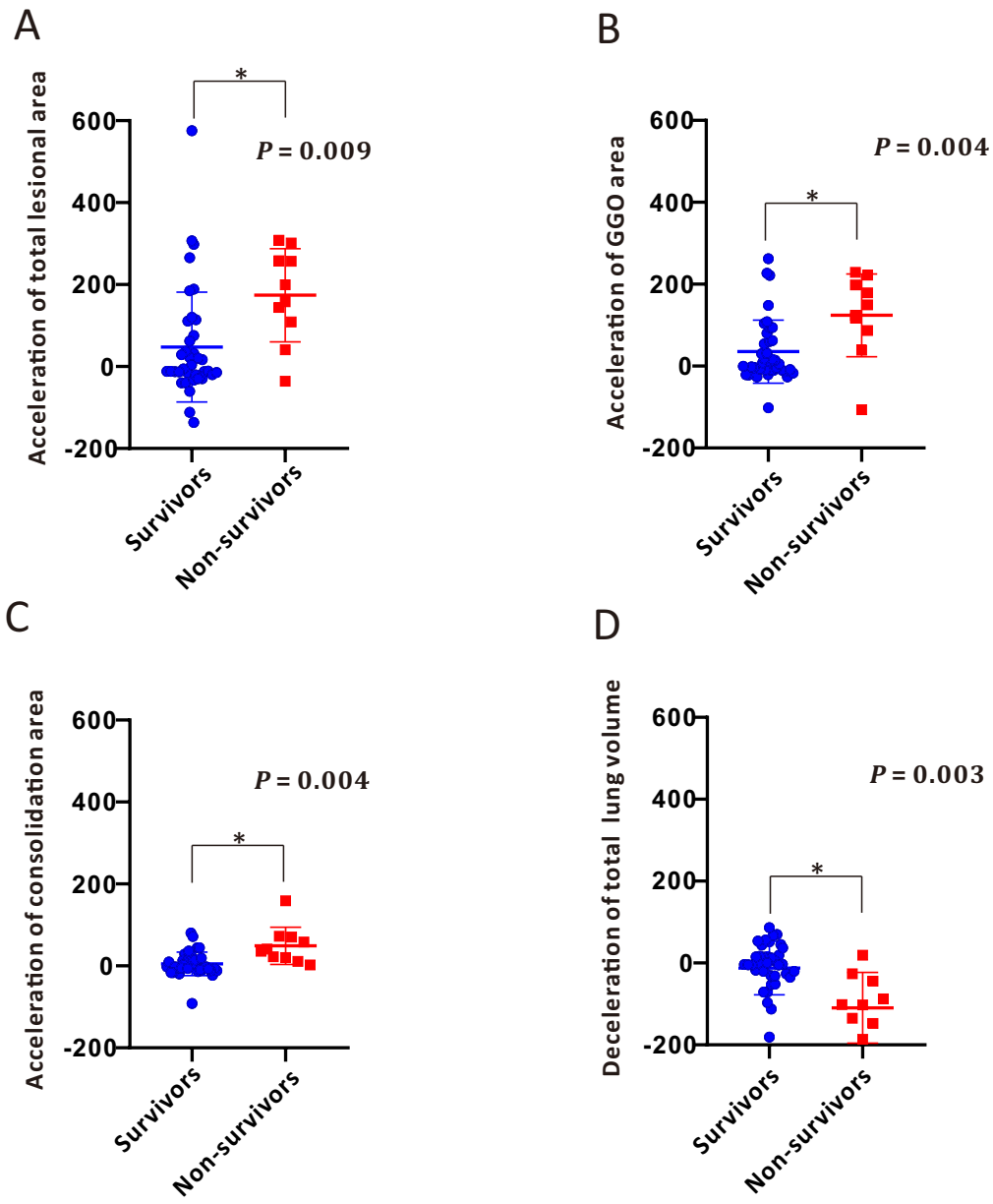
A
Acceleration of total lesional area
600
400
200
0
-200
*
P = 0.009
Survivors
Non-survivors
B
Acceleration of GGO area
600
400
200
0
-200
*
P = 0.004
Survivors
Non-survivors
C
Acceleration of consolidation area
600
400
200
0
-200
*
P = 0.004
Survivors
Non-survivors
D
Deceleration of total lung volume
600
400
200
0
-200
*
P = 0.003
Survivors
Non-survivors

Figure 6

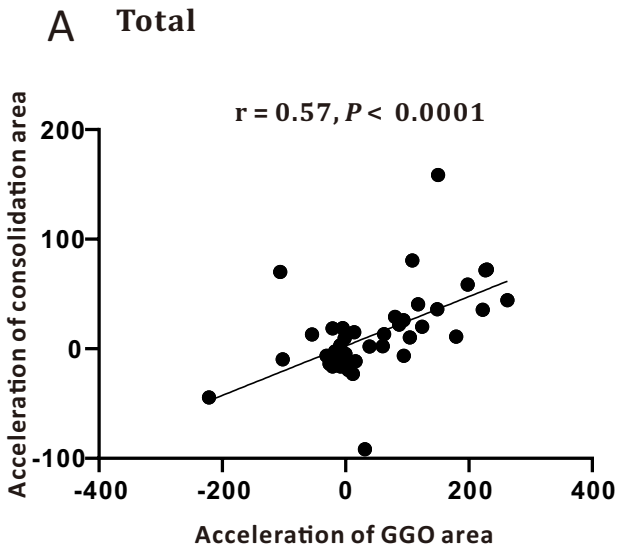
A
Total
r = 0.57, P < 0.0001
Acceleration of consolidation area
Acceleration of GGO area
200
100
0
-100
-400
-200
0
200
400

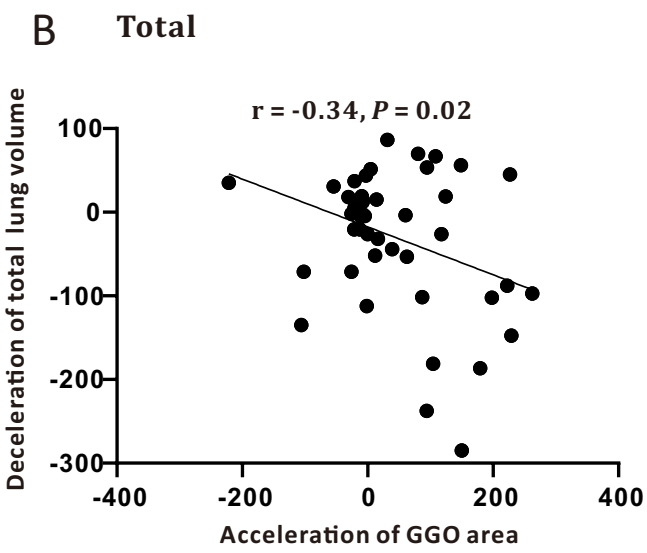
B
Total
r = -0.34, P = 0.02
Deceleration of total lung volume
Acceleration of GGO area
100
0
-100
-200
-300
-400
-200
0
200
400

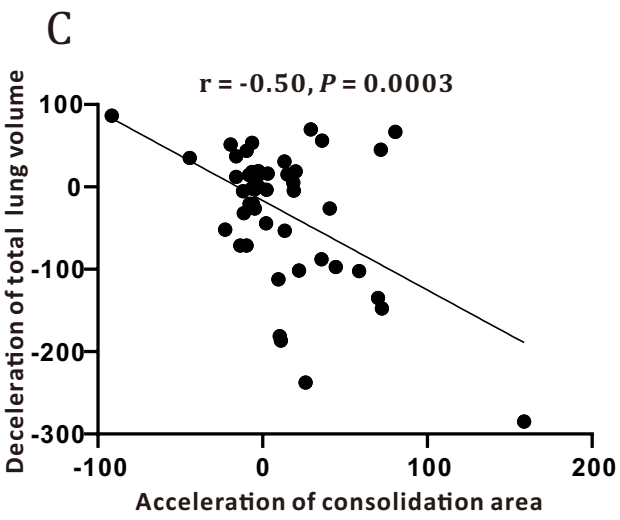
C
r = -0.50, P = 0.0003
Deceleration of total lung volume
Acceleration of consolidation area
100
0
-100
-200
-300
-100
0
100
200

Figure 7

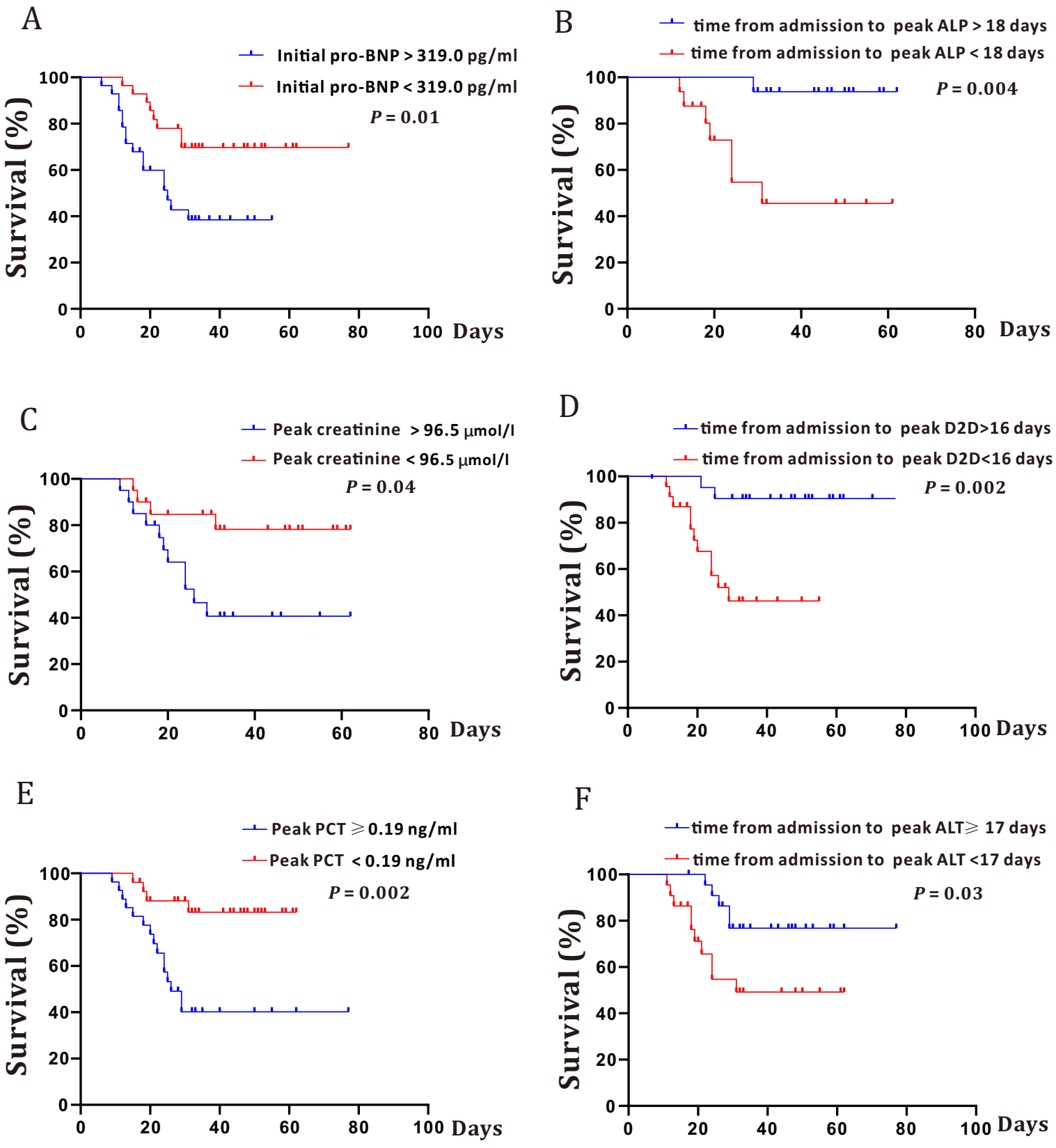
A
Initial pro-BNP > 319.0 pg/ml
Initial pro-BNP < 319.0 pg/ml
P = 0.01
Survival (%)
Days
B
time from admission to peak ALP > 18 days
time from admission to peak ALP < 18 days
P = 0.004
Survival (%)
Days
C
Peak creatinine > 96.5 μmol/l
Peak creatinine < 96.5 μmol/l
P = 0.04
Survival (%)
Days
D
time from admission to peak D2D>16 days
time from admission to peak D2D<16 days
P = 0.002
Survival (%)
Days
E
Peak PCT ⩾ 0.19 ng/ml
Peak PCT < 0.19 ng/ml
P = 0.002
Survival (%)
Days
F
time from admission to peak ALT⩾ 17 days
time from admission to peak ALT <17 days
P = 0.03
Survival (%)
Days

Figure 8

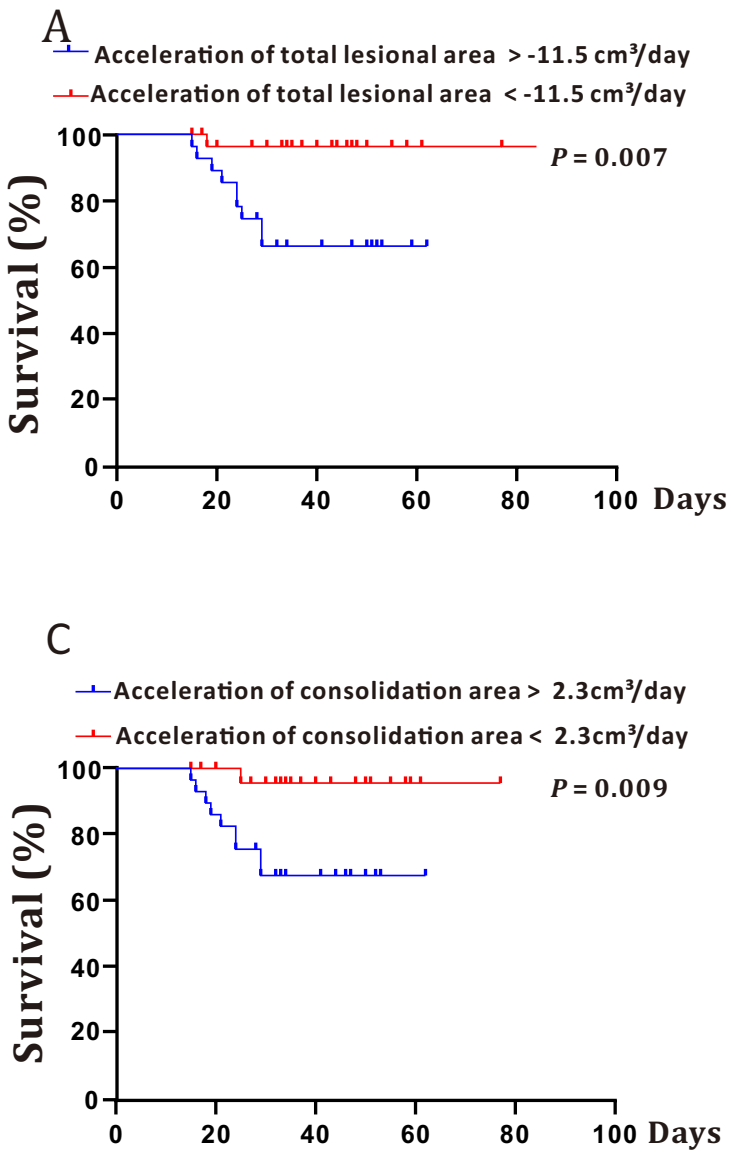
A
Acceleration of total lesional area > -11.5 cm³/day
Acceleration of total lesional area < -11.5 cm³/day
P = 0.007
Survival (%)
100
80
60
40
20
0
0
20
40
60
80
100 Days

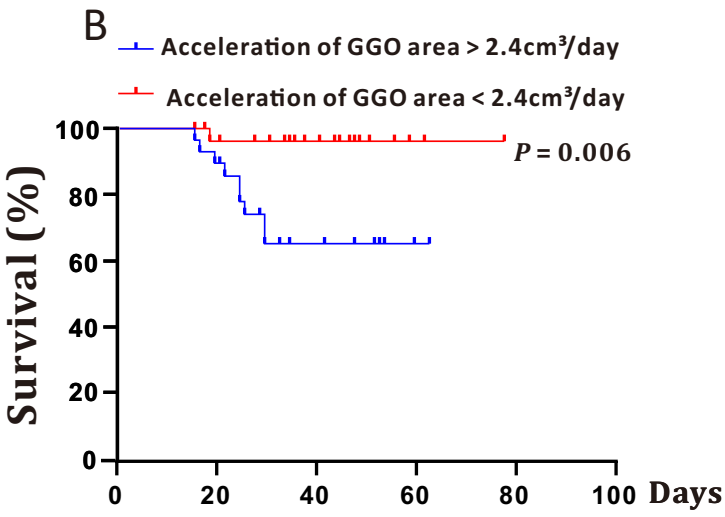
B
Acceleration of GGO area > 2.4cm³/day
Acceleration of GGO area < 2.4cm³/day
P = 0.006
Survival (%)
100
80
60
40
20
0
0
20
40
60
80
100 Days

C
Acceleration of consolidation area > 2.3cm³/day
Acceleration of consolidation area < 2.3cm³/day
P = 0.009
Survival (%)
100
80
60
40
20
0
0
20
40
60
80
100 Days

Figure 9

Supplement

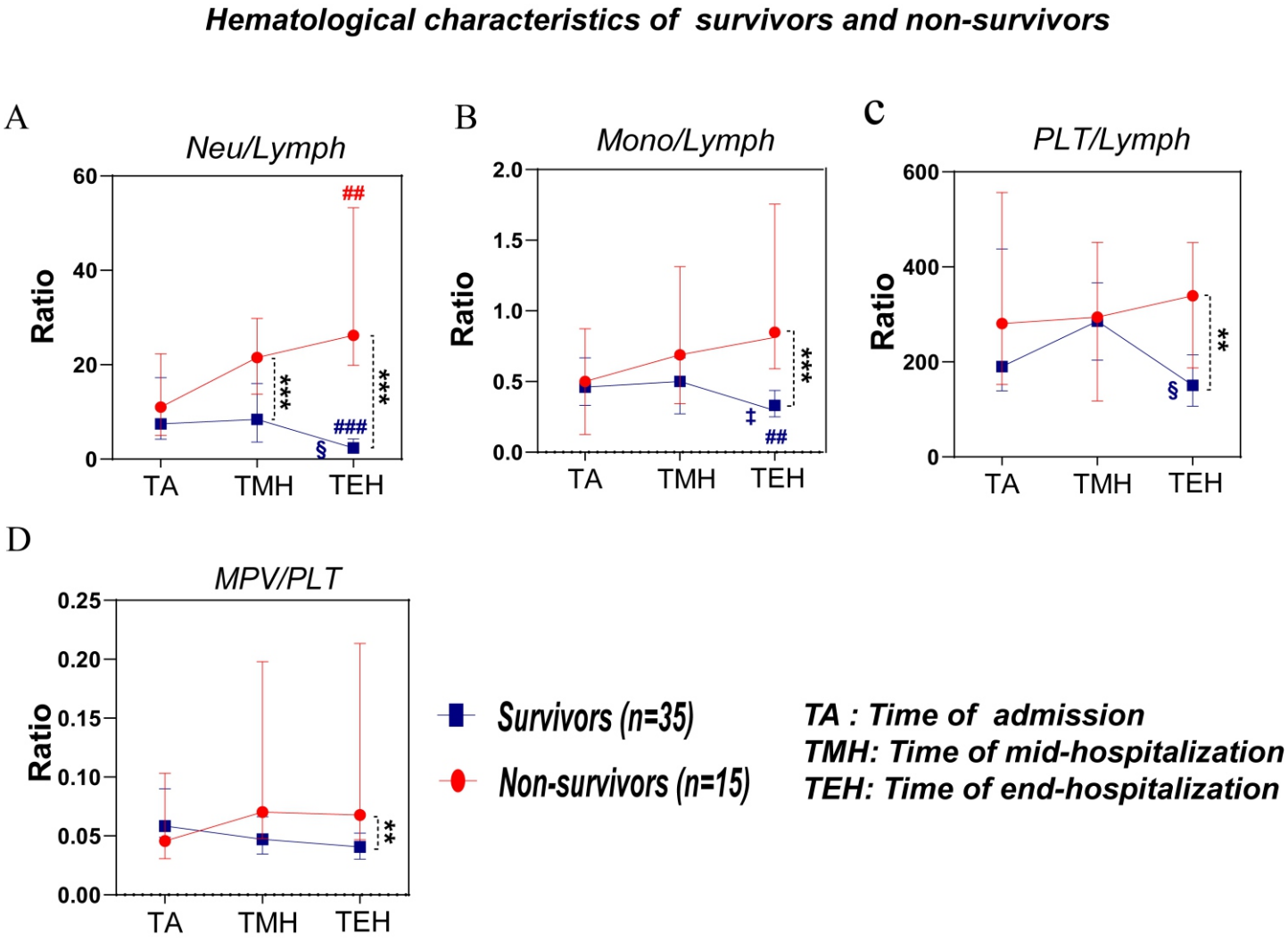

Supplement Figure 1

Table 1 Demographic and clinical features of subjects

	Total	Survivor	Non-survivor	P value
Sample size (%)	67 (100%)	39 (58.2%)	28 (41.8%)	-
Male (%)	41 (61.2%)	24 (61.5%)	17 (60.7%)	0.946
Age (years)	64.4 ± 13.7	63.4 ± 13.3	65.8 ± 14.3	0.300
Exposure of Huanan seafood market	0 (0%)	0 (0%)	0 (0%)	-
Comorbidities (⩾one comorbidity)	45 (67.1%)	23 (60.0%)	22 (78.6%)	0.295
Chronic obstructive pulmonary diseases	1 (1.5%)	0 (0%)	1 (3.6%)	0.234
Hypertension	26 (38.8%)	14 (35.9%)	12 (42.9%)	0.564
Diabetes	16 (23.9%)	8 (20.5%)	8 (28.6%)	0.445
Heart disease	13 (19.4%)	6 (15.4%)	7 (25.0%)	0.326
Carcinoma	3 (4.5%)	1 (2.6%)	2 (7.1%)	0.371
Cerebrovascular diseases	3 (4.5%)	2 (5.1%)	1 (3.6%)	0.761
Other	13 (19.4%)	8 (20.5%)	5 (17.9%)	0.786
Fever	62 (92.5%)	37 (94.9%)	25 (89.3%)	0.391
Cough	57 (85.1%)	34 (87.2%)	23 (82.1%)	0.568
Sputum	41 (61.2%)	25 (64.1%)	16 (57.1%)	0.564
Breathless	54 (80.6%)	31 (79.5%)	23 (82.1%)	0.786
Diarrhea	7 (10.4%)	5 (12.8%)	2 (8.3%)	0.454
Fatigue	32 (47.8%)	21 (53.8%)	11 (39.3%)	0.239
Hypoxemia	64 (95.5%)	36 (92.3%)	28(100%)	0.133
Median time from symptom onset to Hospital discharge (days)	29.0 (18.0-45.0)	41.0 (32.0-50.5)	18.0 (12.0-24.0)	0.000*

Data are n (%) and median (IQR), *P* values were calculated by Mann-Whitney U test, χ^2 test, or Fisher's exact test, as appropriate. * statistical significance.

Table 2 Laboratory analyses of subjects

	Total	Survivor	Non-survivor	P value
Initial FIB, g/L	5.3 ± 6.9	5.8 ± 8.6	4.3 ± 0.9	0.434
Peak of FIB, g/L	4.1 ± 1.6	3.9 ± 1.6	4.6 ± 1.3	0.228
Initial D-dimer, mg/L	3.5 ± 5.0	3.8 ± 1.6	3.0 ± 4.7	0.534
Peak of D-dimer, mg/L	7.3 ± 5.4	6.9 ± 5.3	8.1 ± 5.7	0.506
Initial pro-BNP, pg/ml	1724.7 ± 5001.4	605.6 ± 1093.6	3216.9 ± 7357.6	0.098
Peak of pro-BNP, pg/ml	2912.8 ± 5978.3	1129.2-1407.2	5766.7 ± 8921.5	0.065
Initial PCT, ng/ml	0.5 ± 1.3	0.2 ± 0.4	0.8 ± 1.9	0.110
Peak of PCT, ng/ml	2.8 ± 13.3	0.5 ± 1.7	6.9 ± 21.3	0.222
Initial LDH, IU/L	392.0 ± 184.6	370.8 ± 166.7	420.0 ± 205.6	0.291
Peak of LDH, IU/L	474.2 ± 202.0	430.6 ± 166.7	556.8 ± 240.47	0.026*
Initial creatinine, μmol/L	116.6 ± 173.3	81.7 ± 23.5	165.9 ± 262.3	0.108
Peak of creatinine, μmol/L	188.8 ± 270.9	89.7 ± 24.2	353.9 ± 395.9	0.022*
Initial ALT, u/l	34.1 ± 22.8	32.5 ± 19.3	36.3 ± 27.3	0.512
Peak of ALT, u/l	116.3 ± 247.3	79.1 ± 77.8	175.9 ± 384.9	0.280
Initial AST, u/l	44.3 ± 27.2	40.0 ± 22.0	50.4 ± 32.6	0.152
Peak of AST, u/l	144.9 ± 426.6	57.8 ± 41.4	273.1 ± 658.3	0.172
Initial ALP, u/l	69.0 ± 28.5	67.4 ± 30.6	71.1 ± 25.8	0.607
Peak of ALP, u/l	92.4 ± 41.8	89.5 ± 41.5	97.5 ± 43.4	0.585
Initial TB, μmol/L	11.9 ± 8.6	11.3 ± 5.1	12.6 ± 12.1	0.541
Peak of TB, μmol/L	19.3 ± 13.7	15.7 ± 6.2	24.6 ± 19.6	0.088
Initial DBIL, μmol/l	6.1 ± 7.3	5.6 ± 4.4	6.8 ± 10.2	0.516
Peak of DBIL, μmol/l	8.8 ± 10.6	6.9 ± 6.2	11.3 ± 14.5	0.149
Initial CRP, mg/L	31.0 ± 10.6	28.7 ± 11.7	31.9 ± 8.7	0.279
Peak of CRP, mg/L	31.0 ± 11.3	29.6 ± 13.1	33.4 ± 7.0	0.212
Median time from admission to the peak of D-dimer (Days)	16.0(11.0-21.3)	20.0 (15.5-24.0)	12.0 (9.0-15.0)	0.004*
Median time from admission to the peak of PCT (Days)	12.0(9.0-19.0)	12.5 (7.8-19.3)	12.0 (10.0-18.3)	0.927
Median time from admission to the peak of ALT (Days)	17.0(11.0-24.5)	17.0 (10.0-21.0)	13.0 (11.5-21.5)	0.252
Median time from admission to the peak of ALP(Days)	18.0(9.0-26.0)	19.0 (9.0-23.0)	11.5 (8.8-14.0)	0.107

Data are mean ± SD or median (IQR), FIB= Fibrinogen, BNP=B-type natriuretic peptide, PCT=Procalcitonin, LDH=Lactate dehydrogenase, ALT=Alanine aminotransferase, AST=Aspartate aminotransferase, ALP=Alkaline phosphatase, TB=Total bilirubin, Direct bilirubin=DBIL, CRP=C-reactive protein. *P* values were calculated by Mann-Whitney U test, χ^2 test, or Fisher's exact test, as appropriate. * statistical significance.

Table 3 Treatments of subjects

	Survivor	Non-survivor	P-value
Proportion of BiPAP treatment (%)	34.8% (8/32)	62.5% (15/24)	0.005*
Proportion of Oseltamivir treatment (%)	71.1% (27/38)	64.0% (16/25)	0.556
Proportion of steroid treatment (%)	94.8% (37/39)	89.3% (25/28)	0.910
Total dose of corticosteroid （mg） (normalized to methylprednisolone)	460 （270-670）	240 （100-620）	0.266
Duration of steroid use (Days)	10.0 (6.8-16.0)	7.5 (4.8-12.3)	0.144
Time from initial symptom to the use of steroid (Days)	9.0 (6.0-10.0)	7.5 (5.5-10.8)	0.835

Data are mean ± SD and median (IQR), *P* values were calculated by Mann-Whitney U test, χ^2 test, or Fisher's exact test, as appropriate.

Table 4 Image manifestations of subjects

	Stage 1		Stage 2		Stage 3	
	Survivors	Non-survivors	Survivors	Non-survivors	Survivors	Non-survivors
Patients	19	14	25	12	21	4
Severity （%）						
Mild	2 (10.5%)	4 (28.6%)	0 (0%)	2 (16.7%)	0 (%)	0 (0%)
Moderate	6 (31.6%)	3 (21.4%)	2 (8.0%)	0 (0%)	1 (4.8%)	0(%)
Severe	11 (57.9%)	7 (50.0%)	23 (92.0%)	10 (83.3%)	20(95.2%)	4(100%)
GGO (five lobes involved)	12 （63.2%）	10 (71.4%)	25 (100%)	10 (83.3%)	20 (95.2%)	4 (100%)
Consolidation (at least 2 lobes involved)	6 (31.5%)	3 (21.4%)	13 (52.0%)	4(33.3%)	13 (61.9%)	2 (50%)

Data are percentage (%).